Science of the Total Environment 846 (2022) 157371

Contents lists available at ScienceDirect

Science of the Total Environment

journal homepage: www.elsevier.com/locate/scitotenv

Nanoplastics and ultrafine microplastic in the Dutch Wadden Sea – The hidden plastics debris?

Dušan Materić [a,*], Rupert Holzinger [a], Helge Niemann [b,c]

[a] Institute for Marine and Atmospheric Research Utrecht, Utrecht University, Princetonplein 5, 3584CC Utrecht, the Netherlands
[b] NIOZ Royal Netherlands Institute for Sea Research, Landsdiep 4, 1797 SZ 't Horntje (Texel), the Netherlands
[c] Department of Earth Sciences, Utrecht University, Princetonplein 5, 3584CC Utrecht, the Netherlands

HIGHLIGHTS

- We detected nanoplastics and ultrafine microplastics in the water column of the Dutch Wadden Sea.
- We applied different sampling approaches: direct measurement and preconcentration.
- Using a multi-ion approach, we detected PS and PET nanoplastics in seawater.
- The measured concentration of 4.2 (±2.4) mg PS nanoplastics m^{-3} amounts to 9.8 mg m^{-2}.

GRAPHICAL ABSTRACT

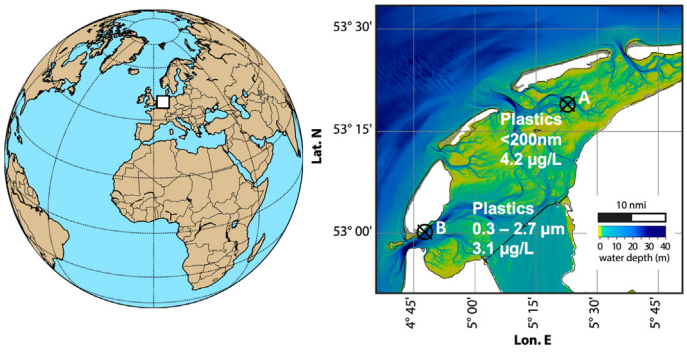

ARTICLE INFO

Editor: Dimitra A Lambropoulou

Keywords:
Nanoplastics
Microplastics
TD-PTR-MS
Polystyrene
Wadden Sea

ABSTRACT

Plastic pollution in the marine environment has been identified as a global problem; different polymer types and fragment sizes have been detected across all marine regions, from sea ice to the equator and the surface to the deep sea. However, quantification of marine plastics debris in the size range of nanoplastics (<1 μm) and ultrafine microplastics (<10 μm) is not constrained, because such minuscule particles are challenging to measure. In this work, we applied a novel analytical assay using Thermal Desorption – Proton Transfer Reaction – Mass Spectrometry (TD-PTR-MS), which is suitable to detect and identify plastics in the nanogram range. From two stations in the Wadden Sea (the Netherlands), we measured nanoplastics directly from seawater aliquots, and from filters with different mesh sizes. Our results show the presence of Polystyrene (PS) and Polyethylene terephthalate (PET) nanopalstics as well as ultrafine microplastics in the Wadden Sea water column. The mass concentration of PS nanoplastics was 4.2 μg/L on average, indicating a substantial contribution of nanoplastics to the Wadden Sea's total plastic budget.

1. Introduction

Large quantities of plastic are released to the ocean with negative consequences to marine life (Wayman and Niemann, 2021). Though ambiguity exists on the importance of the various transport processes through which plastic litter enters the ocean (riverine transport and atmospheric deposition) (González-Fernández et al., 2021; Lebreton et al., 2017; Liss, 2020; Weiss et al., 2021), it is commonly acknowledged that a large fraction of the positively buoyant plastics that have been released to the sea since plastic mass production begun in the 1950s cannot be accounted for (Jambeck et al., 2015; PlasticsEurope, 2019; Wayman and Niemann, 2021). While sedimentation and beaching may explain some removal of plastic marine debris (PMD) from the ocean surface, the 'missing plastic paradox' remains unsolved (Galgani et al., 2021; Koelmans et al., 2017; Onink et al., 2021; van Sebille et al., 2015; Thompson et al., 2004).

Although considered an extremely resilient material, plastics in the ocean fragment into smaller particles, e.g. from macroplastics (>5 mm) to

* Corresponding author.
E-mail address: d.materic@uu.nl (D. Materić).

http://dx.doi.org/10.1016/j.scitotenv.2022.157371
Received 16 March 2022; Received in revised form 6 July 2022; Accepted 10 July 2022
Available online 18 July 2022

microplastics (MP) (1 μm - 5 mm), which may further degrade to nanoplastics (NP) (<1 μm) as a combined result of physical, chemical and biological processes (Dawson et al., 2018; El Hadri et al., 2020; Napper and Thompson, 2019; Wayman and Niemann, 2021). Much of our current knowledge about the abundance of PMD is based on investigating macro and microplastics. However, commonly used protocols for PMD sampling (using plankton nets with mesh sizes of several 100 μm) discriminate against small particles (Lindeque et al., 2020; Poulain et al., 2019; Wayman and Niemann, 2021). Furthermore, identification and quantification of smaller particles are challenging as most of measuring techniques have relatively high detection limits, for example, μFTIR >11 μm, μRaman >0.7 μm (size limit), or > 50 ng (mass limit) per sample for pyrolysis GC–MS (Mintenig et al., 2018; Schwaferts et al., 2019; Sullivan et al., 2020; Velimirovic et al., 2020). Specifically nanoplastics (<1 μm) but also ultrafine microplastics (particles 1–10 μm) are consequently not accounted for in virtually any ocean survey (Ter Halle et al., 2017). The size distribution of marine microplastics is typically skewed towards smaller plastic fragments; e.g. 86 % of surface water and 98 % of sea sediment particles collected in the North Sea are in the size group <100 μm (Lorenz et al., 2019). It is still a matter of debate if this skewness is only related to the number of small particles or the total mass, too (Lebreton et al., 2018). Nevertheless, recent results provide evidence that the total mass of small floating PMD particles (25–1000 μm) could be similar or even higher than the mass of larger items (Poulain et al., 2019), indicating that ultrafine microplastic and nanoplastic could indeed explain an important part of the 'missing plastic paradox'.

In this work, we aimed to analyse nanoplastics and ultrafine microplastics in the Wadden Sea, Netherlands, using a novel TD-PTR-MS method (Materić et al., 2020). Our results provide the first quantitative insights into this overlooked fraction of ocean plastic pollution.

2. Material and methods

2.1. Sampling

Sampling in the Wadden Sea (Site A in Fig. 1) was conducted during a cruise with R/V Navicula on 24-04-2019 at 18:00, 19:00, 20:00 and 21:00 h. Samples were recovered using a 5 L Niskin bottle (made of PVC with PTFE lining) from 1 and 3 m water depth. Aliquots were transferred using silicon tubing attached to the PE faucet of the Niskin bottle after flushing/rinsing the faucet/tube with >1 L of sample water. Aliquots of ~3.5 mL were collected in 4 mL pre-combusted glass vials, which were closed with PTFE lined caps (after caps and vials were rinsed with sample water). Samples were kept dark and cool until analysis. We took field blanks, i.e. Milli-Q water that was exposed to all impurities as the sample water (ie., MQ was filled into the Niskin bottle and tapped through the faucet/tubing into pre-combusted 4 mL vials).

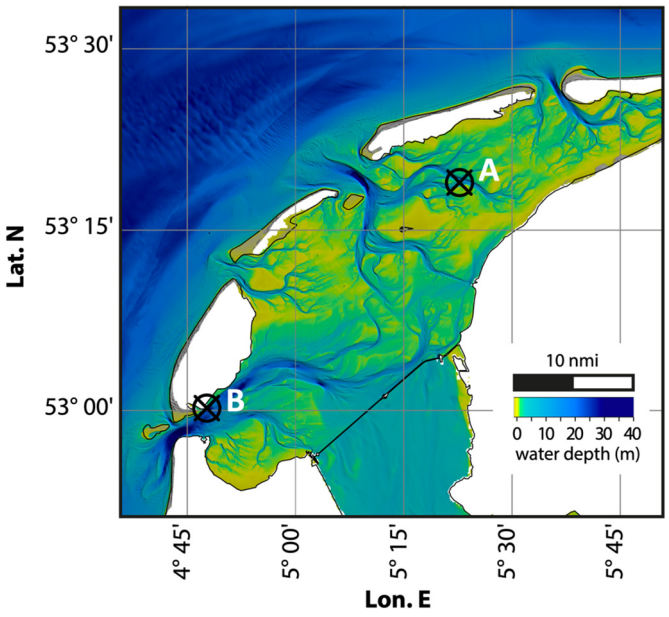

Fig. 1. Sampling sites in the Wadden Sea.

Samples from the NIOZ jetty (Site B in Fig. 1) were collected on 13-07-2020 with a PP bucket from 1 m water depth, poured into pre-combusted 2 L glass bottles and capped with PTFE lined lids, which were pre-rinsed with sample water. In total, 4 time points corresponding to rising tide, high tide, falling tide and ebb tide were sampled. For this campaign, ultra-clean water (HPLC water, VWR Chemicals) was used for the procedural blank as described below.

2.2. Sample preparation

The seawater samples and the field blanks collected from Site A were filtered through PTFE syringe filters (0.2 μm pore size; GE Healthcare, USA) to filter out potential microplastics. A 1 mL aliquot of the filtered sample liquid (containing nanoplastics <200 nm) was then loaded into pre-combusted, transparent 10 mL chromatography vials (VWR, Germany). Field blanks and process blanks (HPLC water) were treated in the same way, thus exposed to the same potential contamination sources as the samples. Then, samples (in duplicate), field blanks and process blanks were dried using a low-pressure evaporation/sublimation system as described earlier (Materić et al., 2017).

For the samples collected at Site B, 1.5 L of each sample was filtered immediately after sampling through 35 mm pre-combusted glass fibre filters (2.7, 1.2, 0.7 μm; Whatmann, 0.3 μm; Advantec). For this purpose, a glass vacuum filtration unit (Millipore) was used. Firstly, the 1.5 L of Wadden Sea sample was filtered through the largest filter size, and the water was collected in a pre-cleaned glass bottle. The filtration unit was then flush three times with HPLC water to remove residual sample water. The next smaller filter size was then mounted on the filter tower, and the sample water that was previously collected was filtered again and collected in a new, pre-cleaned glass bottle. In this way, the filters captured particles with a nominal size of ≥2.7 μm in the first filtration run and 2.7–1.2, 1.2–0.7 and 0.7–0.3 μm in the preceding filtration steps. Prior to each sample filtration, we run procedural blanks of 1.5 L of HPLC grade water (VWR Chemicals) by 'filtering' the water through the system with the same filter meshes. After filtration, all samples and blanks were dried at 50 °C overnight and kept cool and dark until the TD-PTR-MS analysis.

For the analysis, a circular subsample was punched out of the glass fibre filter using a cutting kit made of steel. We subsampled punches of 3 mm diameter from the 2.7 μm filter and 10 mm diameter from all other filters. Hence the filter subsamples correspond to 0.73 % (2.7 μm) and 8.16 % (all others) of the original filter. Thus, each analysis of the cascade filter corresponds to 120 mL of the original 1.5 L sample. Between subsampling, the kit was cleaned with ultrapure water and a cellulose cloth. The punch discs were transferred into clean chromatography vials. Process blanks were treated in the same way.

2.3. Calibration preparation

In order to assess the proton transfer reaction efficiently during thermal desorption and thus to determine the exact concertation of the nanoplastics, we prepared standard sets for calibrating our system for PS and PET analysis. The initial standard for PS was 4 % *v/w* water solution of PS spheres (1 μm in diameter, Microparticles GmbH, Berlin, Germany) from which we made dilutions with the HPLC water resulting in final masses of 10, 25, 50 and 100 ng in the analysis vial.

The PET calibration series was prepared by cutting small punches with an ESM-core sampling toolkit (330 μm inner diameter, Electron Microscopy Sciences, USA) from a PET film (500 nm thick, Goodfellow, UK). Considering a PET density of 1.38 g/cm^3 and a cut-out volume of 4.3 × 10^4 μm^3 per

punched out disc, each disc had a mass of 59 ng. Under a magnifying glass, the discs were manually transferred to the vial with a new metal needle. We obtained a calibration series with 0, 59 (1 disc), 118 (2 discs) and 177 ng (3 disks). All standards were prepared/loaded in pre-combusted 10 mL transparent chromatography vials, and the clean vials exposed to the same environments were used as procedural blanks.

2.4. TD-PTR-MS analysis

We used a modified TD-PTR-MS protocol as described earlier (Materić et al., 2020, 2017). In short, the vials containing samples or blanks were thermally desorbed following the same protocol as described in Materić et al. (2019) (constant at 35 °C for 3 min, then ramp to 350 °C at a rate of 40 °C/min, then constant at 350 °C for 5 min) (Materić et al., 2019). The TD step was performed using zero air stream of 50 mL/min (generated by a catalyser working at 400 °C), while PTR-TOF-MS (PTR8000 Ionicon Analitik, AU, equipped with ion funnel) measured the outflow in real-time (1 Hz resolution). We used the following operation parameters of PTR-TOF-MS: inlet temperature = 180 °C, drift temperature = 120 °C, drift tube pressure = 2.9 mbar, and drift tube voltage = 480 V, resulting in the approximate reduced electric field (E/N) of 120 Td.

2.5. Data analysis

The mass spectra obtained by TD-PTR-MS were extracted using the PTRwid software package (Holzinger, 2015). The signal for each ion was then integrated for 5 min starting when the TD oven temperature reached 200 °C, which reduced the data to one mass spectra per TD run. Each sample was subtracted to the mean filed/procedural blank, and a 3σ detection limit was applied as described earlier (Materić et al., 2019; Materić et al., 2020, 2017). To eliminate the instrument noise and for the contamination evaluation, the filed/procedural blanks were subtracted with the blanks (HPLC water, clean filter for the respective experiment), and the 3σ limit of the detection limit was applied. For the experiments involving PS and PET standards, the samples containing the standards were subtracted to the set of system blanks (clean vials) obtained in the same experiment, and a 3σ detection limit was also applied as above.

2.5.1. Fingerprinting the plastics signal

Resulting mass spectra of samples field/procedural blanks were analysed for plastic fingerprints as explained in our previous works (Materić et al., 2022, 2021, 2020). In brief, for the plastic identification, we used 40 ions from the plastics library available with the software and set the m/z tolerance to 0.05 Da (an example of plastic ions fingerprinting is illustrated in Fig. A.1). We accepted the positive fingerprint if the algorithm score was above 2σ compared to 1000 synthetic spectra (z-score = 2, $p < 0.025$) (Materić et al., 2021, 2020). The fingerprint algorithm's output with calculated loads is summarised in Table A.1 (details of the fingerprint outputs can be found in SI).

2.5.2. Quantification

TD-PTR-MS measurements yield concentrations of numerous organic ions present in the sample, which is estimated from known reaction rates during proton transfer reactions (Holzinger, 2015). The concentrations of organic ions are calculated according to the following formula (Cappellin et al., 2012; Hansel et al., 1995; Jordan et al., 2009):

$$[C] = \frac{1}{kt} \times \frac{[M \cdot H^+]}{[H_3O^+]}$$

where $[C]$ is concentration, k is reaction rate coefficient, t the residence time of the primary ions in the drift tube, $[M{\cdot}H^+]$ and $[H_3O^+]$ are ion counts representing the protonated analyte and primary ions corrected for the transmission (Holzinger et al., 2019). Such calculated concentrations are considered semi-quantitative, because they represent the amount of organic matter that is actually ionised in the system. As the PTR ionization efficiency of organics is not 100 % (there are losses in neutral molecular fragments and CO_2 – not detected by the PTR-MS) the semi-quantitative values can be considered as the minimum amount – lower threshold of the actual ion concentrations (Materić et al., 2020).

Thus, we calculated the calibration coefficients for the 40-ion fingerprint approach followed by the semi-quantification:

$$k_{NP} = \frac{[c]NP_L}{[c]NP_M}$$

where $[c]NP_L$ is the loaded quantity of nanoplastics in ng, and $[c]NP_M$ the semi-quantitatively measured nanoplastics concertation in ng using the 40-ion fingering approach described above (Materić et al., 2020).

The correction factors for the nanoplastics detected, k_{PS} and k_{PET} can be used to convert semi-quantitative data to full-quantitative NP concentrations, in the linear part of the calibration curve (up to a load of ~80 ng, Fig. 2). However, for better accuracy, we determined calibration formulae from regression analysis, and we considered a linear (PS) and polynomial (PET) fit based on the 40 ions, as shown in the Fig. 2.

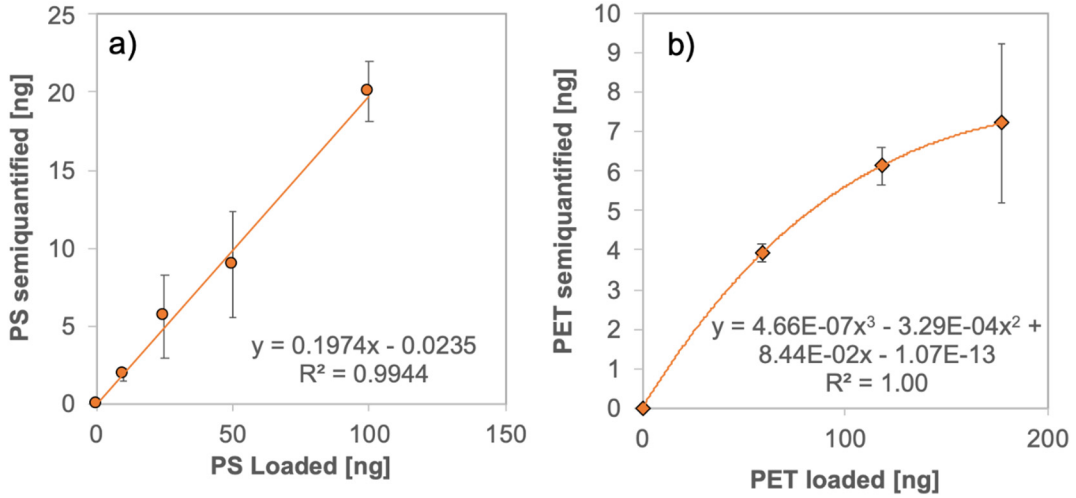

Fig. 2. TD-PTR-MS sensitivity plot based on the 40-ion approach for a) PS and b) PET. Note PS has linear and PET polynomial response. No plastics traces were found in the blanks. Error bars represent SD of replicates. Our semiquantitative measurements of environmental nanoplastics were on average 13.4 (range 0–28) ng for PS, and 1.2 ng for PET (range 0–4.8) in a TD run (see the SI).

For PS nanoplastics, the response was linear (Fig. 2a). Irrespective of the sample loads, the correction factor k_{PS} remained hence constant at 5.28 ± 1.48. However, for PET, the correction factor increased with an increase in loaded PET; from k_{PET} = 15.05 ± 0.9 for 59 ng load to 26.06 ± 6.8 for 177 ng load. This increase in k_{PET} (and the polynomial distribution) could be explained by inefficient thermal desorption and ionization when a larger quantity of comparably big particles was loaded. Note that our measured quantities of environmental nanoplastics (i.e. semiquantitative for filter samples) were on average 13.4 ng per sample for PS (range 0–28 ng, two samples measured ~28 ng), and 1.2 ng per sample for PET (range 0–4.8 ng per sample) (see the SI). The semiquantitative loads for the direct measurement was on average 1.6 ng in a sample (ranging 0–3.5 ng) (see the SI).

2.5.3. Detection limit estimation

In line with our previous works (Materić et al., 2019; Materić et al., 2020, 2017), the theoretical detection limits were calculated considering ions m/z 105.07 and m/z 123.04 for PS and PET, respectively, based on 3σ of the blanks. Note that these were calculated based on virgin plastics; thus, no interference from other polymers was present. The detection limits for all ions are reported in the SD (see the Data availability section).

The detection limit for PS and PET was 0.001 and 0.063 ng/mL, respectively when preconcentration was applied, and 0.12 and for 7.69 ng/mL when directly measuring (PS and PET, respectively). Concentrations measured in our seawater samples were in the range 0.1–6.5 ng/mL for PS and 0.1–2.8 ng/mL for PET (Table A.1).

2.6. Quality control

TD-PTR-MS and the nanoplastics analysis approach showed good prevention of false-positive and false-negative results. For instance, overestimation was prevented by 1) a strict fingerprinting algorithm that examines multiple ions, which are the product of a typical plastic-type generated in and stored in a library (e.g. 40 most expressed ions emitted during thermal desorption of a plastic) (Materić et al., 2021, 2020); 2) a sample preparation protocol that includes a low-pressure evaporation step where many volatile and semi-volatile organic compounds from the natural matrix are lost (Materić et al., 2022, 2021, 2017); 3) a slow thermal desorption process that facilitates thermal separation of the organics according to their boiling points monitored in real-time (every second) by a high-resolution (4000 FWHM) and high-sensitivity PTR-ToF-MS (<1 ppt range in the generated gas stream (Lindinger et al., 1998)) and 4) postprocessing quantification algorithm that prevent potential anomalous overexpression of expected ions (all in details explained in our previous work (Materić et al., 2020)). Together, these exclude false-positive detection due to the potential presence of plastic monomers. For example, styrene, which has a boiling point of 145 °C, would not affect our results as we considered compounds (mass spectra) only after the temperature of the TD unit reached 200 °C (i.e., potentially present monomers would be lost in the early part of slow thermal desorption). Also, other matrix artefacts (for example styrene-like or other ions, coming from natural polymers at a similar boiling point as the plastics) would be identified and removed in our postprocessing routine which considers multiple ions (fingerprint) for identification (Materić et al., 2022, 2020).

To prevent sample contamination, glass and metal labware was precombusted, or if not possible, cleaned with ultrapure water, and, for samples, rinsed with the sample water.

However, certain procedures were not possible without using plastics materials. This included micropipettes, pipetting tips (PE), syringes (PE, rubber), filters and filter holders (PE, PTFE/Teflon), bottle/vial seals (PTFE). However, in blank runs we could not find that the high-quality labware described above released substantial amounts of nanoplastics. I.e., in direct seawater measurement (Site A), we could not detect any traces of nanoplastics in the field blanks (see the SI), yet we detected traces of PS and PP/PPC (4.7 and 3.1 ng/L semi-quantitative loads, respectively) in the procedural blanks from side B. However, the traces of PS are negligible as they are ~54 times lower compared to the average concentrations measured in samples from that side (254.6 ng/L, semi-quantitative loads). No PET, PE or PVC traces were detected in the blanks. In other words, filtering of 1.5 L of water provides useful preconcentration where loads of nanoplastics detected in the samples were significantly higher ($p = 6.9 \times 10^{-8}$, one-tail distribution, unequal variances) than traces found in the blanks.

A higher level of the contamination as we found in the blanks of the cascade-filtering experiment, compared to the direct seawater measurement, can be explained by extensive procedures involved in such method (filtering, drying, cutting, transferring), which might result in higher contact with the potential contamination sources (longer exposure to the air, additional equipment used etc.).

3. Results

In this work, we applied two sampling strategies to quantify the seawater concentration of nanoplastics and small microplastic at two Wadden Sea sites. The samples form Site A (Fig. 1) were taken at two depths (1 and 3 m), repeatedly every hour over a time period of 4 h during rising tide (4 samples per depth in total). These were analysed directly by TD-PTR-MS (1 mL load) without pre-concentration (Materić et al., 2021, 2020) and we found PS nanoplastics with an average concentration of 4.5 (±3.0) and 3.8 (±1.7) μg/L at 1 and 3 m water depth, respectively (Fig. 3, Table A.1). The concentration measured at the different depths appeared not to be significantly different (paired t-test, $p = 0.69$, note the small number of samples); the mean concentration of PS nanoplastics throughout the water column was thus 4.2 μg/L (range: 0.1–6.5 μg/L). Other types of nanoplastics polymers (PE, PP, PET or PVC) were not detected using the strict fingerprinting approach explained in our earlier work (Materić et al., 2020).

Assuming a spherical particle geometry with a diameter of 200 nm (upper size of the filter pores used to separate microplastics from nanoplastics) and a density of 1 g/cm^3 for PS, we calculated a minimum number concentration of 1.03×10^9 nanoplastic particles per litre of seawater.

The surface water samples from the Site B (Fig. 1) were sampled at 1 m depth over 24 h, thus covering a full tidal cycle. The water samples from this side were processed in a cascade filter setup (mesh sizes: 2.7, 1.2, 0.7 and 0.3 μm) aiming to pre-concentrate nanoplastics and ultrafine microplastics. Our measurements showed the presence of PS and PET ultrafine micro- and nanoplastics (Fig. 4 and Table A.1).

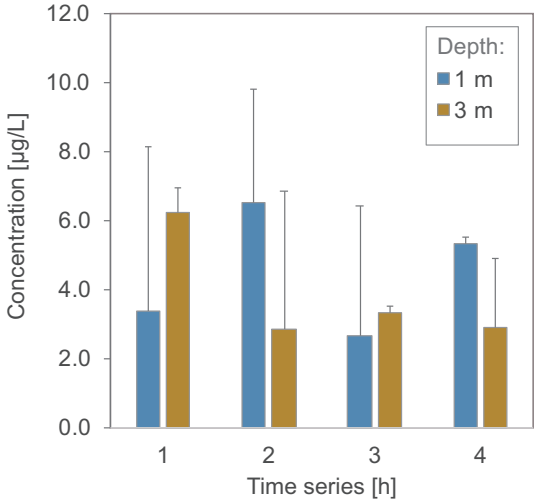

Fig. 3. Time series of polystyrene nanoplastic (size <200 nm) concentration measured in the Wadden Sea at different depth (direct seawater measurements). Error bars represent SD of replicates. Large error bars for the surface samples 1–3 and for the 3 m depth sample 3 come as nanoplastics have been detected in one replica but not the other (see the details in Table A.1 and supplementary data).

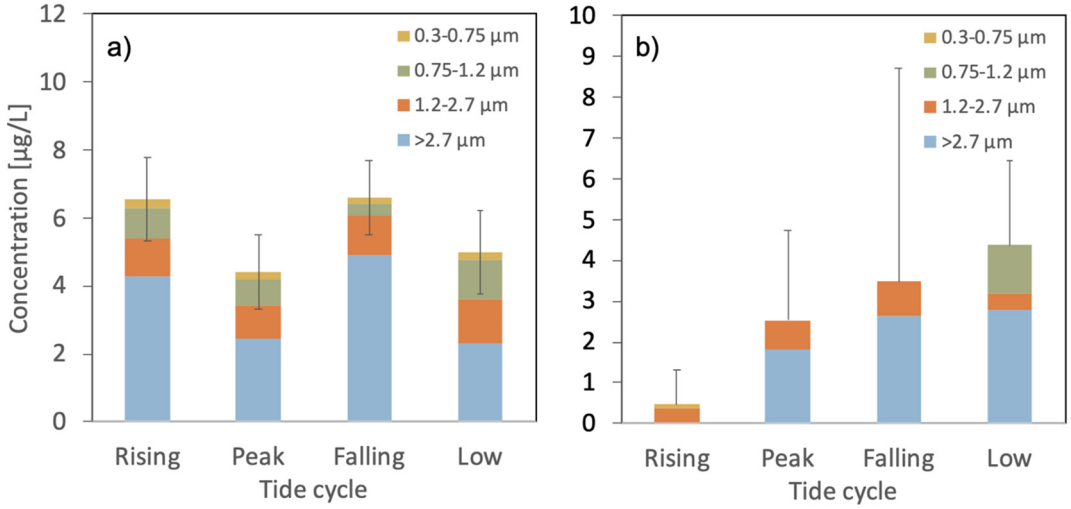

Fig. 4. Nanoplastics concentration change during the tidal cycle measured with cascade filtering set up a) PS and b) PET. The particle size cut-off points of the filter stages are indicated. Error bars represent SD of the replicates for all size fractions.

The average concentration of plastics (sum of both polymers: PS and PET) measured on the filter with a mesh size of 2.7 µm was 5.3 µg/L, and for the ultrafine and nano particles (0.3–2.7 µm), it was 3.1 µg/L. We did not analyse nanoplastic concentrations in the seawater passing the last stage of the cascade filtration (0.3 µm).

4. Discussion

4.1. Comparison between NP and MP loads

This study provides first quantitative results of environmental nanoplastics (PS and PET) in the Wadden Sea, and to our knowledge in any marine region. The average mass concentration of our measurements of PS nanoplastics was 4.2 µg/L (see the Quantification section). For comparison, an average number concentration of 27.2 microplastic particles m^{-3} mostly in the size range < 100 µm has been reported for southern North Sea surface waters (Lorenz et al., 2019) (the southern North Sea is in close vicinity to the Wadden Sea). Considering average particle sizes of 200 and 500 µm (which is more conservative than <100 µm reported from the southern North Sea – e.g. particles 50 µm would yield less mass), spherical shape, and a density of 1 g/cm^3, the mass of one microplastic particle amounts to 4.2 and 65.4 µg, respectively. The reported number density in the North Sea of almost 800 particles per m^2 (2.7 microplastic particles per m^2 at the sea surface and 797 particles per m^2 of sea sediment) (Lorenz et al., 2019), amounts to 3.3 or 52.3 mg m^{-2}, when considering particle sizes of 200 and 500 µm, respectively. Our results of 4.2 mg PS m^{-3} (measured directly) amounts to 9.8 mg m^{-2} considering an average Wadden Sea water depth of 2.34 m. Assuming that microplastic concentrations in the Wadden Sea are similar to the North Sea, our results suggest that the total mass of PS nanoplastics is in a similar magnitude order as microplastics, indicating a substantial contribution of nanoplastics to the Wadden Sea's total plastic's budget.

The importance of nano- and ultrafine microplastics determined from direct measurements is further corroborated by the cascade filter experiment at Site B. There, we can compare the loads of microplastics >2.7 µm (retained by our first filter in the cascade) with the size fraction <2.7 µm (the rest of the filters in the cascade), which comprises ultrafine microplastics and nanoplastics. The mass of ultrafine PS microplastics and nanoplastics (the fraction <2.7 µm) was on average 2.2 µg/L, while the mass of larger microplastics retained by 2.7 µm filter was 3.5 µg/L. This shows that ultrafine microplastics and nanoplastic contributes 38.5 % of all plastic particles at the time of our sampling. Note that our cascade filtering method cannot be used to determine size group distributions because we expect that a filter with a given nominal mesh size also retains particles smaller than the nominal mesh size. Hence, the 2.7 µm filter will, at least to some degree, retain nanoplastics and nanoplastics aggregates as well.

Commonly detected microplastics types found in the southern North sea are PE, PP and PS with a lot variability between close-by stations (Lorenz et al., 2019). Although we found PS in all our samples, we did not detect PE or PP, which we cannot fully explain. Previously, we detected PE NP during the analysis of virgin plastics and we found PE and PP nanoplastics in Alpine snow, firn core Greenland and Antarctic sea ice samples (Materić et al., 2022, 2021, 2020). However, there is a large knowledge gap in understanding the natural mechanisms of NP formation, transportation, hetero-aggregation and sedimentation, which might be differential for the various types of plastic types.

4.2. Upscaling to the sea surface and the total Wadden Sea

Our results give the first indications for the presence and concentration of NPs and ultrafine MPs, i.e. the fine-fraction of marine plastics debris that has remained unobserved in previous investigations. Nevertheless, our results have limitations, as we did not cover a wide array of geographically distributed stations and the temporal resolution of our measurements is relatively small. The upscaling of NP and ultrafine MP concentrations (Table 1) should hence be considered cautiously.

The Dutch Wadden Sea extends for ~2200 km^2 (landward of the barrier islands) and based on publicly available bathymetry data ("Westelijke Waddenzee (bathymetric maps)," 2013) the harmonized average water depth is 2.34 m and the total volume is 5.14 km^3 on average. Assuming a non-clustered distribution of PS nanoplastics, then our average measurements of 4.2 µg/L PS NP <200 nm at Site A integrated over 2.34 m water depth amount to 9.8 mg/m^2, or 21.6 tons upscaled to the entire surface area of the Dutch Wadden Sea (Table 1).

Similarly calculated from our cascade filter measurement, PS and PET microplastics >2.7 µm (to tentatively 1 mm - no visible particles/fibres were observed on the filter) amounted to 3.5 µg/L and 1.8 µg/L, respectively. This is equivalent to 8.2 and 4.2 mg/m^2 and thus 18.0 and 9.3 tons of PS and PET microplastics in the Dutch Wadden Sea, respectively. However, for the fraction <2.7 µm, which combines ultrafine microplastics and nanoplastics, we measured PS and PET loads of 2.2 and 0.9 µg/L – equivalent to 5.1 and 2.1 mg/m^2. The total mass of these ultrafine plastics

Table 1
Concentrations of nanoplastics, ultrafine microplastics and microplastics, surface concentrations and total content in the Dutch Wadden Sea (assuming average 4 m depth and surface area of 2300 km^2). More details on the concentrations for each sample can be found in Appendix Table A.1.

Sample origin	Size range [nm]	Type of plastics	Average concentration [μg/L]	Concentration range [μg/L]	Surface concentration [mg/m^2]	Quantity in the Dutch Wadden Sea [tons]
Site A	<200	PS	4.2	2.7–6.5	9.8	21.6
Site B	300–2700	PS	2.2	1.7–2.7	5.1	11.3
Site B	300–2700	PET	0.9	0.5–1.6	2.1	4.6
Site B	>2700	PS	3.5	2.3–4.9	8.2	18.0
Site B	>2700	PET	1.8	0–2.8	4.2	9.3

particles (0.3–2.7 μm) in the Dutch Wadden Sea is 11.3 and 4.6 tons, PS and PET, respectively (Table 1).

4.3. Sources and spatiotemporal distribution of PS and PET nanoplastics

PS is a common polymer and used globally as insulation material and for single-use items such as coffee cups, food containers and optical disc packing. Similarly, PET is a common polymer that is widely used for producing bottles as well as fibres, e.g. for clothing. Both PS and (though to a lesser degree) PET macro and microplastics are commonly found in the ocean, including the southern North Sea (Lorenz et al., 2019). The PS and PET NP detected here might thus originate from PS/PET debris (macro and micro plastic) that has been fragmented further to nanometre sized particles as a result of UV-radiation, mechanical stress and biological action (Wayman and Niemann, 2021). In addition, the NPs might also originate from terrestrial sources. To the best of our knowledge, the only available literature data on NP concentrations in aquatic systems are from the river Tawe (Wales, UK) where PS nanoplastic concentrations of 242 μg/L were measured (Sullivan et al., 2020). This indicates that rivers could be an important transport vector, at least for PS NP. NPs, including PS and PET, have also have been measured in alpine snow (Materić et al., 2021, 2020), and atmospheric transport of ultrafine microplastics has been found, too (Allen et al., 2019; Bergmann et al., 2019; Brahney et al., 2020; Dris et al., 2016; Ross et al., 2021). In fact, aeolian deposition of MP in the sea was estimated to account for 10 Mt yr^{-1} (Liss, 2020), which is similar to earlier estimates of plastic waste inputs from land to sea, that do not consider atmospheric deposition (Jambeck et al., 2015). Hence, at least to some degree, the NP levels detected here might originate from atmospheric fallout.

We observed that PS NP concentrations show temporal concentration patterns corresponding to the tidal regime (Fig. 4a). It is also notable that the relative concentration of different size groups behaves differently (Fig. A.2). For Site B, we found that the concentration of PS (all size fractions) during rising and falling tides were significantly higher than during peak and low tide (ANOVA, $p = \ll 0.001$; pairs Low-Falling $p = 0.0059$, Peak-Falling $p = 0.0008$, Low-Rising $p = 0.0068$ and Peak-Rising $p = 0.0009$, Figs. 4a and A.3). Nevertheless, we also noticed that PET concertation increases during the full tidal cycle (Fig. 4b). This change in PET concentrations, which is uncoupled from PS loads (Fig. 4a), tentatively indicates different mixing processes for these two NP types. We suggest that PS nanoplastics might be resuspended from sediments during rising and falling tide when current velocities are high (in comparison to slack tide). PET on the other hand might sediment to a lesser degree than PS, possibly related to the atmospheric input followed by differential aggregation behaviour in the water column. Clearly, a deeper understanding of NP sources and NP behaviour in the water column as well as a higher spatiotemporal resolution of nanoplastic concentrations is needed.

4.4. Toxicity implications

The concentrations of environmental nanoplastics present in the Wadden Sea samples were <10 μg/L for PS and < 5 μg/L for PET. Ecotoxicological studies have so far only been conducted with PS nanoplastics and typically at much higher levels (often ~100 mg/L), yet some works investigated NP concentrations similar to those that we observed in the Wadden Sea. For example, the swimming speed of green alga and rotifers was reduced at PS NP concentrations of 1 μg/L (Kögel et al., 2020). The composition of exopolymeric substances of a diatom changed to higher protein-carbohydrate ratios at 0.1 μg/L, though a significant decrease in survival was only found at 100,000 μg/L (Shiu et al., 2020). Growth and aggregation properties of two dinoflagellates that are symbionts of corals was reduced at PS NP concentrations of 10, 100 and 10,000 μg/L, which may negatively affect uptake of the symbionts by the coral host (Ripken et al., 2020). These findings suggest that marine life in the Wadden Sea could already be affected by nanoplastics.

4.5. Nanoplastics quantification improvement

Quantification of nanoplastics in environmental samples has been recognised as a unique challenge (Mintenig et al., 2018; Schwaferts et al., 2019; Velimirovic et al., 2020). In previous work, we presented a semiquantitative approach to measure nanoplastics using TD-PTR-MS, which showed potential for estimating concentrations of nanoplastics in environmental samples (Materić et al., 2021, 2020). The semiquantitative approach is particularly important for polymer types that do not yet have available analytical standards that can be used for calibration (only PS NP standards are commercially available). However, the semiquantitative approach is associated with lower threshold values of the NP concentrations in the sample, underestimated for the ionization efficiency.

Here, for the first time, we developed a fully quantitative TD-PTR-MS method for PS and PET nanoplastics (Fig. 2), however this does not account for the uncertainties in filtering efficiency (experiment at Site B).

4.6. Limitations of this study

We only found PS nanoplastics, but not PET, using direct measurements from seawater, while pre-concertation onto quartz filters revealed the presence of PS and PET and was associated to a higher reproducibility and a >100-fold lower detection limit. Though we did not directly compare the two methods on one sample set, it seems likely that the direct measurement could simply not resolve the relatively low PET concentrations in the water column. The higher sensitivity when applying cascade filtering is probably related to the relatively high amount of sample water concentrated on a filter (i.e., 1.5 L per filter; corresponding to 11 mL per subsection used for a single measurement for the filtering stage >2.7 μm, and 120 mL for all the other stages) when compared to the direct measurements (1 mL seawater used for measurements).

Future sensitivity improvement should be approached from different angles, both procedural and instrumental. Our work indicates that preconcertation steps lower the detection limit. On the other hand, we argue that more steps in the sampling/extraction protocol bear the risk of contamination, which brings a new limit of the method (see Quality control in Material and methods section for details). The digestion protocols of organics or different extraction temperatures should be examined further as

they might increase signal over matrix noise. On the other hand, upgraded with more sensitive PTR-MS technology (such as ion funnel (Brown et al., 2017)) our method improved the detection limit by 44 % and the ionization efficiency ('recovery') of PS by 20 % compared to the previous results (Materić et al., 2020).

In this work, we used a relatively small seawater volume for analysis (mL or L for Sites A and B, respectively). Handling small volumes is advantageous because of logistics in the field and it allows high-throughput measurements. However, volumes of millilitres might not be sufficient to provide a comparison between total nanoplastics and microplastics mass concentrations. The reason is that most of the size classes of microplastics (e.g. >500 μm) are typically low in abundance (<0.027 microplastics fragments per litre of southern North Sea surface water) but comprise a relatively large total mass compared to the sub-micrometre sized particles (Lorenz et al., 2019). This might also explain why we measured somewhat comparable plastics loads using different sampling methods as most of the plastic on the filter was nanoplastic and ultrafine microplastics (we could not observe any particles by naked eye).

We found indications that variations in nanoplastics and ultrafine microplastic concentrations could be driven by tidal forces. However, we did not analyse sediment samples, which could shed light on the exchange of NP and ultrafine MP between seabed and seawater. Future method optimization towards sediment sample analysis should be considered in order to address the role of sea sediment as a sink and reservoir for seawater nanoplastics.

5. Conclusions

In this work, we demonstrate the presence of PS and PET nano plastics as well as ultrafine microplastics in the water column of the Dutch Wadden Sea. In comparison to measuring NPs directly in sea water aliquots, a better detection of the plastics was achieved with a more complex sampling/preconcentration approach (cascade filtering), but this approach also introduced more procedure-related contamination. We further improved the TD-PTR-MS method for plastic trace analysis and obtained ionization efficiency rates, which allowed us to quantify PS and PET. In the center of the Wadden Sea, an average of 4.2 μg/L PS nanoplastics <200 nm integrated over depth amounted to 9.8 mg/m^2, or 21.6 tons when upscaled to the entire surface area of the Dutch Wadden Sea. This implies that nano plastics contribute substantially to the total plastic budget in this environment and calls for further research in this field.

Data availability

All data needed to evaluate the conclusions in the paper (including raw files, the scripts and processing stages of the data analysis) are available at https://surfdrive.surf.nl/files/index.php/s/EM8n2uPNtGwWhHE (readme.doc has the file descriptions).

Upon the revision, we will upload it to the permanent repository YODA (https://public.yoda.uu.nl), and it will be assigned a DOI.

All data needed to evaluate the conclusions in the paper (including raw files, the scripts and processing stages of the data analysis) are available at https://doi.org/10.24416/UU01-A9A28C.

CRediT authorship contribution statement

DM designed the experiment with the help of HN and RH. HN performed the sampling. DM performed the analysis and data processing and wrote the manuscript with feedback from all co-authors.

Declaration of competing interest

The authors declare no competing interests.

Acknowledgements

DM and RH acknowledge support from Dutch Research Council (Nederlandse Organisatie voor Wetenschappelijk Onderzoek – NWO) project "Nanoplastics: hormone- mimicking and inflammatory responses?" (grant number OCENW.XS2.078), and project "Plastic Air" (grant number OCENW.XS.066). HN acknowledges NWO project "How much Nanopalstic is in the Ocean" (grant number OCENW.XS2.018) and the European Research Council for ERC-CoG Grant No. 772923, project VORTEX. This publication was supported through the UPlasticS3 network (https://www.uu.nl/en/research/sustainability/uplastics3). We thank students Sophie ten Hietbrink and Grant Francis for participating in some TD-PTR-MS analyses as well as captain, crew and scientific parties of the relevant cruises with R/V Navicula.

Appendix A

Table A.1
Nanoplastics concentrations in the Wadden Sea samples. *, **, *** represent z-score of >2, 3, 4, respectively.

Sample name	Sample type	Fraction size	Tide cycle	Site	Depth [m]	PS [μg/L]	SD	Match conf.	PET [μg/L]	SD	Match conf.
WS29	Seawater	<200 nm	Rising	A	1	3.4	4.8	*	–	–	–
WS30	Seawater	<200 nm	Rising	A	1	6.5	3.3	***	–	–	–
WS31	Seawater	<200 nm	Rising	A	1	2.7	3.8	**	–	–	–
WS32	Seawater	<200 nm	Rising	A	1	5.4	0.2	***	–	–	–
WS29	Seawater	<200 nm	Rising	A	3	6.3	0.7	***	–	–	–
WS30	Seawater	<200 nm	Rising	A	3	2.8	4.0	**	–	–	–
WS31	Seawater	<200 nm	Rising	A	3	3.3	0.2	**	–	–	–
WS32	Seawater	<200 nm	Rising	A	3	2.9	2.0	***	–	–	–
WS_2.7_R	Quartz filter	>2.7 μm	Rising	B	1	4.3	0.7	***	–	–	–
WS_2.7_P	Quartz filter	>2.7 μm	Peak	B	1	2.4	0.6	***	1.8	1.6	*
WS_2.7_F	Quartz filter	>2.7 μm	Falling	B	1	4.9	0.6	***	2.6	4.5	*
WS_2.7_L	Quartz filter	>2.7 μm	Low	B	1	2.3	0.4	***	2.8	0.2	*
WS_1.2_R	Quartz filter	1.2 to 2.7 μm	Rising	B	1	1.1	0.2	***	0.4	0.6	*
WS_1.2_P	Quartz filter	1.2 to 2.7 μm	Peak	B	1	1.0	0.2	***	0.7	0.6	*
WS_1.2_F	Quartz filter	1.2 to 2.7 μm	Falling	B	1	1.2	0.2	***	0.9	0.7	*
WS_1.2_L	Quartz filter	1.2 to 2.7 μm	Low	B	1	1.3	0.4	***	0.4	0.7	*
WS_0.75_R	Quartz filter	0.75 to 1.2 μm	Rising	B	1	0.9	0.1	***	–	–	–
WS_0.75_P	Quartz filter	0.75 to 1.2 μm	Peak	B	1	0.8	0.2	***	–	–	–
WS_0.75_F	Quartz filter	0.75 to 1.2 μm	Falling	B	1	0.4	0.1	***	–	–	–
WS_0.75_L	Quartz filter	0.75 to 1.2 μm	Low	B	1	1.2	0.2	***	1.2	1.2	*
WS_0.3_R	Quartz filter	0.3 to 0.75 μm	Rising	B	1	0.3	0.2	***	0.1	0.2	*
WS_0.3_P	Quartz filter	0.3 to 0.75 μm	Peak	B	1	0.2	0.1	***	–	–	–
WS_0.3_F	Quartz filter	0.3 to 0.75 μm	Falling	B	1	0.2	0.1	***	–	–	–
WS_0.3_L	Quartz filter	0.3 to 0.75 μm	Low	B	1	0.2	0.1	***	–	–	–

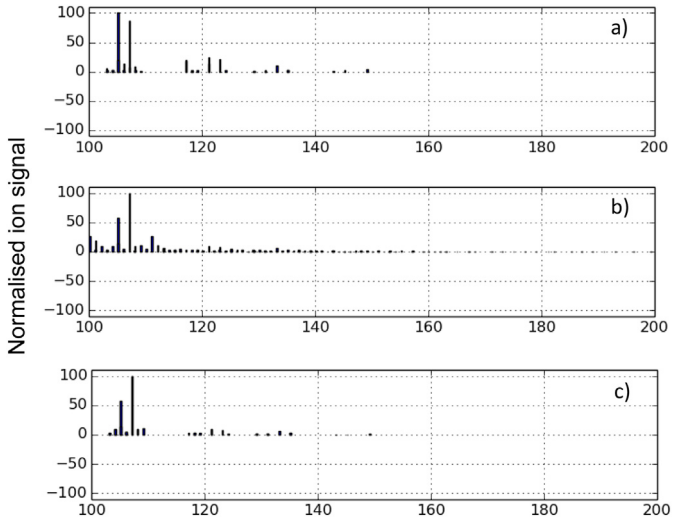

Fig. A.1. Fingerprinting PS micro/nanoplastics in a sample (match confidence '***', z-score > 4), a) ions in PS library, b) mass spectra of a sample (WS_1.2_L), c) PS nanoplastics signal in the same sample (WS_1.2_L). The signals are normalised to the highest peak. The fingerprint algorithm, scoring and evaluation were in details addressed in our previous work (Materić et al., 2020).

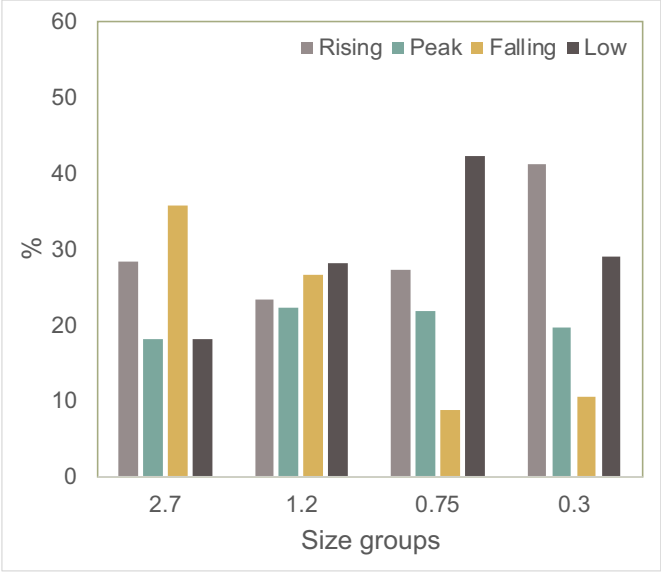

Fig. A.2. Mixing dynamic of ultrafine micro- and nanoplastics over a tidal cycle measured with cascade filtering set up.

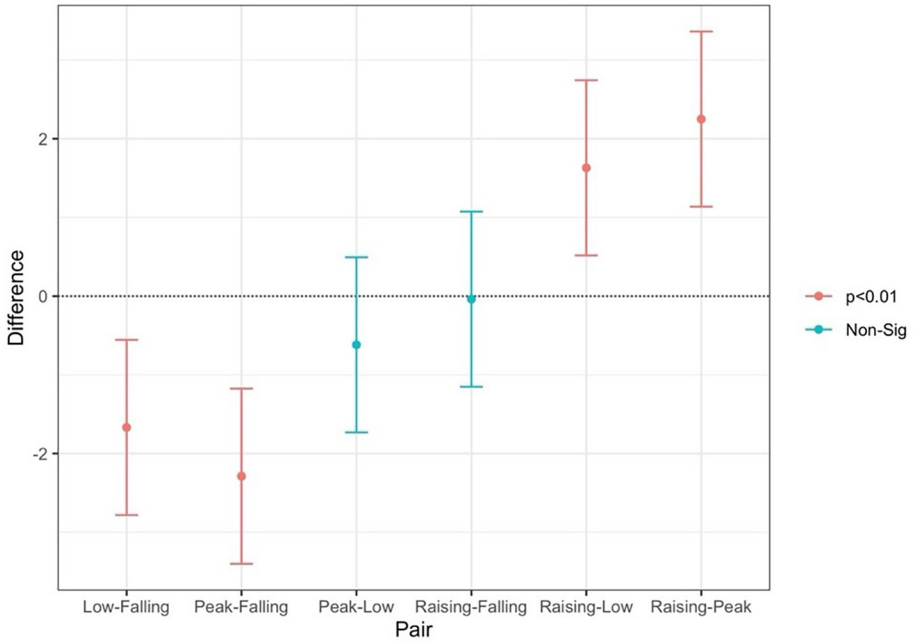

Fig. A.3. Difference in the nanoplastics concentration over a tidal cycle. ANOVA and Tukey post hoc test indicate the significance between Low-Falling ($p = 0.0059$) Peak-Falling ($p = 0.0008$), Low-Rising ($p = 0.0068$) and Peak-Rising ($p = 0.0009$) pairs.

References

Allen, S., Allen, D., Phoenix, V.R., Roux, G.L., Jiménez, P.D., Simonneau, A., Binet, S., Galop, D., 2019. Atmospheric transport and deposition of microplastics in a remote mountain catchment. Nat. Geosci. 1. https://doi.org/10.1038/s41561-019-0335-5.

Bergmann, M., Mützel, S., Primpke, S., Tekman, M.B., Trachsel, J., Gerdts, G., 2019. White and wonderful? Microplastics prevail in snow from the Alps to the Arctic. Sci. Adv. 5, eaax1157. https://doi.org/10.1126/sciadv.aax1157.

Brahney, J., Hallerud, M., Heim, E., Hahnenberger, M., Sukumaran, S., 2020. Plastic rain in protected areas of the United States. Science 368, 1257–1260. https://doi.org/10.1126/science.aaz5819.

Brown, P.A., Cristescu, S.M., Mullock, S.J., Reich, D.F., Lamont-Smith, C.S., Harren, F.J.M., 2017. Implementation and characterization of an RF ion funnel ion guide as a proton transfer reaction chamber. Int. J. Mass Spectrom. 414, 31–38. https://doi.org/10.1016/j.ijms.2017.01.001.

Cappellin, L., Karl, T., Probst, M., Ismailova, O., Winkler, P.M., Soukoulis, C., Aprea, E., Märk, T.D., Gasperi, F., Biasioli, F., 2012. On quantitative determination of volatile organic compound concentrations using proton transfer reaction time-of-flight mass spectrometry. Environ. Sci. Technol. 46, 2283–2290. https://doi.org/10.1021/es203985t.

Dawson, A.L., Kawaguchi, S., King, C.K., Townsend, K.A., King, R., Huston, W.M., Nash, S.M.B., 2018. Turning microplastics into nanoplastics through digestive fragmentation by Antarctic krill. Nat. Commun. 9, 1001. https://doi.org/10.1038/s41467-018-03465-9.

Dris, R., Gasperi, J., Saad, M., Mirande, C., Tassin, B., 2016. Synthetic fibers in atmospheric fallout: a source of microplastics in the environment? Mar. Pollut. Bull. 104, 290–293. https://doi.org/10.1016/j.marpolbul.2016.01.006.

El Hadri, H., Gigault, J., Maxit, B., Grassl, B., Reynaud, S., 2020. Nanoplastic from mechanically degraded primary and secondary microplastics for environmental assessments. NanoImpact 17, 100206. https://doi.org/10.1016/j.impact.2019.100206.

Galgani, F., Brien, A.S., Weis, J., Ioakeimidis, C., Schuyler, Q., Makarenko, I., Griffiths, H., Bondareff, J., Vethaak, D., Deidun, A., Sobral, P., Topouzelis, K., Vlahos, P., Lana, F., Hassellov, M., Gerigny, O., Arsonina, B., Ambulkar, A., Azzaro, M., Bebianno, M.J., 2021. Are litter, plastic and microplastic quantities increasing in the ocean? Microplast. Nanoplast. 1, 2. https://doi.org/10.1186/s43591-020-00002-8.

González-Fernández, D., Cózar, A., Hanke, G., Viejo, J., Morales-Caselles, C., Bakiu, R., Barceló, D., Bessa, F., Bruge, A., Cabrera, M., Castro-Jiménez, J., Constant, M., Crosti, R., Galletti, Y., Kideys, A.E., Machitadze, N., Pereira de Brito, J., Pogojeva, M., Ratola, N., Rigueira, J., Rojo-Nieto, E., Savenko, O., Schöneich-Argent, R.I., Siedlewicz, G., Suaria, G., Tourgeli, M., 2021. Floating macrolitter leaked from Europe into the ocean. Nat. Sustain. 4, 474–483. https://doi.org/10.1038/s41893-021-00722-6.

Hansel, A., Jordan, A., Holzinger, R., Prazeller, P., Vogel, W., Lindinger, W., 1995. Proton transfer reaction mass spectrometry: on-line trace gas analysis at the ppb level. Int.J.Mass Spectrom.Ion Process., Honour Biography David Smith 149–150, 609–619. https://doi.org/10.1016/0168-1176(95)04294-U Honour Biography David Smith.

Holzinger, R., 2015. PTRwid: a new widget tool for processing PTR-TOF-MS data. Atmos. Meas. Tech. 8, 3903–3922. https://doi.org/10.5194/amt-8-3903-2015.

Holzinger, R., Acton, W.J.F., Bloss, W.J., Breitenlechner, M., Crilley, L.R., Dusanter, S., Gonin, M., Gros, V., Keutsch, F.N., Kiendler-Scharr, A., Kramer, L.J., Krechmer, J.E., Languille, B., Locoge, N., Lopez-Hilfiker, F., Materić, D., Moreno, S., Nemitz, E., Quéléver, L.L.J., Sarda Esteve, R., Sauvage, S., Schallhart, S., Sommariva, R., Tillmann, R., Wedel, S., Worton, D.R., Xu, K., Zaytsev, A., 2019. Validity and limitations of simple reaction kinetics to calculate concentrations of organic compounds from ion counts in PTR-MS. Atmos. Meas.Tech. 12, 6193–6208. https://doi.org/10.5194/amt-12-6193-2019.

Jambeck, J.R., Geyer, R., Wilcox, C., Siegler, T.R., Perryman, M., Andrady, A., Narayan, R., Law, K.L., 2015. Plastic waste inputs from land into the ocean. Science 347, 768–771. https://doi.org/10.1126/science.1260352.

Jordan, A., Haidacher, S., Hanel, G., Hartungen, E., Märk, L., Seehauser, H., Schottkowsky, R., Sulzer, P., Märk, T.D., 2009. A high resolution and high sensitivity proton-transfer-reaction time-of-flight mass spectrometer (PTR-TOF-MS). Int. J. Mass Spectrom. 286, 122–128. https://doi.org/10.1016/j.ijms.2009.07.005.

Koelmans, A.A., Kooi, M., Law, K.L., van Sebille, E., 2017. All is not lost: deriving a top-down mass budget of plastic at sea. Environ. Res. Lett. 12, 114028. https://doi.org/10.1088/1748-9326/aa9500.

Kögel, T., Bjorøy, Ø., Toto, B., Bienfait, A.M., Sanden, M., 2020. Micro- and nanoplastic toxicity on aquatic life: determining factors. Sci. Total Environ. 709, 136050. https://doi.org/10.1016/j.scitotenv.2019.136050.

Lebreton, L., Slat, B., Ferrari, F., Sainte-Rose, B., Aitken, J., Marthouse, R., Hajbane, S., Cunsolo, S., Schwarz, A., Levivier, A., Noble, K., Debeljak, P., Maral, H., Schoeneich-Argent, R., Brambini, R., Reisser, J., 2018. Evidence that the Great Pacific Garbage Patch is rapidly accumulating plastic. Sci. Rep. 8, 4666. https://doi.org/10.1038/s41598-018-22939-w.

Lebreton, L.C.M., van der Zwet, J., Damsteeg, J.-W., Slat, B., Andrady, A., Reisser, J., 2017. River plastic emissions to the world's oceans. Nat. Commun. 8, 15611. https://doi.org/10.1038/ncomms15611.

Lindeque, P.K., Cole, M., Coppock, R.L., Lewis, C.N., Miller, R.Z., Watts, A.J.R., Wilson-McNeal, A., Wright, S.L., Galloway, T.S., 2020. Are we underestimating microplastic abundance in the marine environment? A comparison of microplastic capture with nets of different mesh-size. Environ. Pollut. 265, 114721. https://doi.org/10.1016/j.envpol.2020.114721.

Lindinger, W., Hansel, A., Jordan, A., 1998. On-line monitoring of volatile organic compounds at pptv levels by means of proton-transfer-reaction mass spectrometry (PTR-MS) medical applications, food control and environmental research. Int. J. Mass Spectrom. Ion Process. 173, 191–241. https://doi.org/10.1016/S0168-1176(97)00281-4.

Liss, P.S., 2020. Microplastics: all up in the air? Mar. Pollut. Bull. 153, 110952. https://doi.org/10.1016/j.marpolbul.2020.110952.

Lorenz, C., Roscher, L., Meyer, M.S., Hildebrandt, L., Prume, J., Löder, M.G.J., Primpke, S., Gerdts, G., 2019. Spatial distribution of microplastics in sediments and surface waters of the southern North Sea. Environ. Pollut. 252, 1719–1729. https://doi.org/10.1016/j.envpol.2019.06.093.

Materić, D., Kasper-Giebl, A., Kau, D., Anten, M., Greilinger, M., Ludewig, E., van Sebille, E., Röckmann, T., Holzinger, R., 2020. Micro- and nanoplastics in alpine snow: a new method for chemical identification and (semi)quantification in the nanogram range. Environ. Sci. Technol. 54, 2353–2359. https://doi.org/10.1021/acs.est.9b07540.

Materić, D., Kjær, H.A., Vallelonga, P., Tison, J.-L., Röckmann, T., Holzinger, R., 2022. Nanoplastics measurements in Northern and Southern polar ice. Environ. Res. 208, 112741. https://doi.org/10.1016/j.envres.2022.112741.

Materić, D., Ludewig, E., Brunner, D., Röckmann, T., Holzinger, R., 2021. Nanoplastics transport to the remote, high-altitude Alps. Environ. Pollut. 117697. https://doi.org/10.1016/j.envpol.2021.117697.

Materić, D., Ludewig, E., Xu, K., Röckmann, T., Holzinger, R., 2019. Brief communication: Analysis of organic matter in surface snow by PTR-MS – implications for dry deposition dynamics in the Alps. Cryosphere 13, 297–307. https://doi.org/10.5194/tc-13-297-2019.

Materić, D., Peacock, M., Kent, M., Cook, S., Gauci, V., Röckmann, T., Holzinger, R., 2017. Characterisation of the semi-volatile component of dissolved organic matter by thermal desorption – proton transfer reaction – mass spectrometry. Sci. Rep. 7, 15936. https://doi.org/10.1038/s41598-017-16256-x.

Mintenig, S.M., Bäuerlein, P.S., Koelmans, A.A., Dekker, S.C., van Wezel, A.P., 2018. Closing the gap between small and smaller: towards a framework to analyse nano- and microplastics in aqueous environmental samples. Environ. Sci.: Nano 5, 1640–1649. https://doi.org/10.1039/C8EN00186C.

Napper, I.E., Thompson, R.C., 2019. Environmental deterioration of biodegradable, oxo-biodegradable, compostable, and conventional plastic carrier bags in the sea, soil, and open-air over a 3-year period. Environ. Sci. Technol. 53, 4775–4783. https://doi.org/10.1021/acs.est.8b06984.

Onink, V., Jongedijk, C.E., Hoffman, M.J., van Sebille, E., Laufkötter, C., 2021. Global simulations of marine plastic transport show plastic trapping in coastal zones. Environ. Res. Lett. 16, 064053. https://doi.org/10.1088/1748-9326/abecbd.

PlasticsEurope, 2019. Plastics - The Facts 2019.

Poulain, M., Mercier, M.J., Brach, L., Martignac, M., Routaboul, C., Perez, E., Desjean, M.C., ter Halle, A., 2019. Small microplastics as a main contributor to plastic mass balance in the North Atlantic subtropical gyre. Environ. Sci. Technol. 53, 1157–1164. https://doi.org/10.1021/acs.est.8b05458.

Ripken, C., Khalturin, K., Shoguchi, E., 2020. Response of coral reef dinoflagellates to nanoplastics under experimental conditions suggests downregulation of cellular metabolism. Microorganisms 8, 1759. https://doi.org/10.3390/microorganisms8111759.

Ross, P.S., Chastain, S., Vassilenko, E., Etemadifar, A., Zimmermann, S., Quesnel, S.-A., Eert, J., Solomon, E., Patankar, S., Posacka, A.M., Williams, B., 2021. Pervasive distribution of polyester fibres in the Arctic Ocean is driven by Atlantic inputs. Nat. Commun. 12, 106. https://doi.org/10.1038/s41467-020-20347-1.

Schwaferts, C., Niessner, R., Elsner, M., Ivleva, N.P., 2019. Methods for the analysis of submicrometer- and nanoplastic particles in the environment. TrAC Trends Anal. Chem. 112, 52–65. https://doi.org/10.1016/j.trac.2018.12.014.

Shiu, R.-F., Vazquez, C.I., Chiang, C.-Y., Chiu, M.-H., Chen, C.-S., Ni, C.-W., Gong, G.-C., Quigg, A., Santschi, P.H., Chin, W.-C., 2020. Nano- and microplastics trigger secretion of protein-rich extracellular polymeric substances from phytoplankton. Sci. Total Environ. 748, 141469. https://doi.org/10.1016/j.scitotenv.2020.141469.

Sullivan, G.L., Gallardo, J.D., Jones, E.W., Hollliman, P.J., Watson, T.M., Sarp, S., 2020. Detection of trace sub-micron (nano) plastics in water samples using pyrolysis-gas chromatography time of flight mass spectrometry (PY-GCToF). Chemosphere 249, 126179. https://doi.org/10.1016/j.chemosphere.2020.126179.

Ter Halle, A., Jeanneau, L., Martignac, M., Jardé, E., Pedrono, B., Brach, L., Gigault, J., 2017. Nanoplastic in the North Atlantic subtropical gyre. Environ. Sci. Technol. 51, 13689–13697. https://doi.org/10.1021/acs.est.7b03667.

Thompson, R.C., Olsen, Y., Mitchell, R.P., Davis, A., Rowland, S.J., John, A.W.G., McGonigle, D., Russell, A.E., 2004. Lost at sea: where is all the plastic? Science 304. https://doi.org/10.1126/science.1094559 838-838.

van Sebille, E., Wilcox, C., Lebreton, L., Maximenko, N., Hardesty, B.D., van Franeker, J.A., Eriksen, M., Siegel, D., Galgani, F., Law, K.L., 2015. A global inventory of small floating plastic debris. Environ. Res. Lett. 10, 124006. https://doi.org/10.1088/1748-9326/10/12/124006.

Velimirovic, M., Tirez, K., Voorspoels, S., Vanhaecke, F., 2020. Recent developments in mass spectrometry for the characterization of micro- and nanoscale plastic debris in the environment. Anal. Bioanal. Chem. https://doi.org/10.1007/s00216-020-02898-w.

Wayman, C., Niemann, H., 2021. The fate of plastic in the ocean environment – a minireview. Environ. Sci.: Process.Impacts https://doi.org/10.1039/D0EM00446D.

Weiss, L., Ludwig, W., Heussner, S., Canals, M., Ghiglione, J.-F., Estournel, C., Constant, M., Kerhervé, P., 2021. The missing ocean plastic sink: gone with the rivers. Science 373, 107–111. https://doi.org/10.1126/science.abe0290.

Westelijke Waddenzee (bathymetric maps), 2013 Westelijke Waddenzee (bathymetric maps), 2013. doi:10.4121/uuid:717d2e38-9ce7-423f-947d-7c74567dafd8